Bioconjugate Chemistry

Article

pubs.acs.org/bc

Photoregulating RNA Digestion Using Azobenzene Linked Dumbbell Antisense Oligodeoxynucleotides

Li Wu,[†,‡] Yujian He,*[,†,‡] and Xinjing Tang*[,‡]

[†]School of Chemistry and Chemical Engineering, University of Chinese Academy of Sciences, Beijing 100049, China

[‡]State Key Laboratory of Natural and Biomimetic Drugs, School of Pharmaceutical Sciences, Peking University, Beijing 100191, China

Supporting Information

ABSTRACT: Introduction of 4,4′-bis(hydroxymethyl)-azobenzene (azo) to dumbbell hairpin oligonucleotides at the loop position was able to reversibly control the stability of the whole hairpin structure via UV or visible light irradiation. Here, we designed and synthesized a series of azobenzene linked dumbbell antisense oligodeoxynucleotides (asODNs) containing two terminal hairpins that are composed of an asODN and a short inhibitory sense strand. Thermal melting studies of these azobenzene linked dumbbell asODNs indicated that efficient *trans* to *cis* photoisomerization of azobenzene moieties induced large difference in thermal stability (ΔT_m = 12.1−21.3 °C). In addition, photomodulation of their RNA binding abilities and RNA digestion by RNase H was investigated. The *trans*-azobenzene linked asODNs with the optimized base pairs between asODN strands and inhibitory sense strands could only bind few percentage of the target RNA, while it was able to recover their binding to the target RNA and degrade it by RNase H after light irradiation. Upon optimization, it is promising to use these azobenzene linked asODNs for reversible spatial and temporal regulation of antisense activities based on both steric binding and RNA digestion by RNase H.

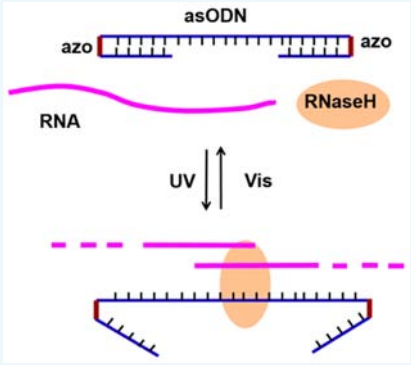

INTRODUCTION

Antisense oligodeoxynucleotides (asODNs) have been proven effective in gene silencing in many experimental systems and are being developed as treatments for cancer and other diseases in human clinical trials.[1,2] Hybridization of an antisense oligodeoxynucleotide to a target mRNA inhibits translation by sterically blocking the ribosome with formation of asODN/mRNA duplex, and/or recruiting endogenous ribonucleases with activation of RNase H-mediated hydrolysis of mRNA in mammalian cells.[3,4] Thus, effective asODNs can silence disease genes that are caused by the expression of an abnormal gene or the overexpression of a normal gene.[5−7] Light-activated methods with high spatial and temporal resolution would permit the inhibition or reduction of gene expression in a cell or tissue-specific fashion and thereby limit systemic toxicity.[8−15] Remote control over structures and activities of nucleic acids has been achieved by employing photoresponsive molecules introduced in diverse structural positions, including phosphate backbone,[16−18] nucleobases,[19−23] ribose moiety,[24,25] and nucleoside surrogates[26−29] in native nucleic acids. Thus, the introduction of these photoresponsive units in nucleic acid molecules has been explored and established in diverse applications, for instance, inhibition of duplex formation, control of gene transcription, regulation of aptamer recognition, manipulation of enzyme activities, and gene expression. And yet, more photoregulation strategies are focused on introduction of photolabile molecules that could be irreversibly removed by light irradiation,[8−17,19,30−33] for instance, coumarin and *o*-nitrobenzyl. Striking examples were presented by Dmochowski and Tang et al.[31−33] using a short complementary sense strand as the blocking moiety for an asODN with a heterobifunctional photocleavable linker. This represents one of the efficient methods for photomodulating RNase H-mediated RNA digestion.

Azobenzene has served as the excellent choice since the photoinduced reversible *trans*−*cis* isomerization of azobenzenes is accompanied by a large change in geometry and the considerable impact on structures and activities of nucleic acids.[34−36] Pioneering works related to photoswitchable nucleic acids were achieved by Komiyama, Asanuma, and co-workers.[26,27,37−41] This method has been generally applied as the installation of the azobenzene unit into a sequence as an additional nucleoside. Azobenzene intercalates between the neighboring pairing bases in the *trans* form. Following irradiation, the *cis*-azobenzene reduced its ability to intercalate in ODN duplexes, thus destabilizing the duplexes. A thorough thermodynamic study on position and number of incorporated azobenzenes has been performed as well.[37,38] As a pioneering example, photoregulation of RNase H assay was achieved with azobenzene-tethered DNA.[40,41] With this system, incorporation of multiple azobenzene moieties in DNA sense strands or DNAzyme was able to control the DNA/RNA or DNA/DNA

Received: March 5, 2015
Revised: May 6, 2015
Published: May 11, 2015

DOI: 10.1021/acs.bioconjchem.5b00125
Bioconjugate Chem. 2015, 26, 1070−1079

hybridization to regulate target RNA digestion through azobenzene photoisomerization. However, for ODNs modified with multiple azobenzene moieties, the long irradiation time was required to generate the fully active molecule. In fact, prolonged UV irradiation would lead to side effects, such as cell toxicity.

Based on many biological activities of nucleic acids that involve the hybridization between DNA and RNA, we have sought to develop synthetically facile and high-quantum-efficiency routes for reversibly photomodulating the hybridization of asODNs to target RNA molecules. In the previous reports,[42,43] 4,4′-bis(hydroxymethyl)azobenzene has been reported to replace the loop nucleotides in a hairpin DNA, which is able to control the stability of whole hairpin structure reversibly via UV or visible light irradiation. Furthermore, when 4,4′-bis(hydroxymethyl)azobenzene was introduced to the loop of ODN hairpins with 4, 5, and 6 paired nucleobases as hairpin stems, the thermodynamic stability of the ODN hairpins decreased sharply from *trans* to *cis* conformation.

In this study, a series of azobenzene linked dumbbell asODNs were designed and synthesized with antisense strand complementary to target RNA and two terminal hairpin structures, in which 4,4′-bis(hydroxymethyl)azobenzene replaced both hairpin loops. In the *trans* form of azobenzene loops, more stable hairpins were formed, and thereby the antisense ODN strands were temporally sequestered. UV irradiation induced the distortion of azobenzene at the loop position of the hairpin and destabilized ODN hairpins, allowing asODN fragments to hybridize their complementary target RNA. Once the duplex of the antisense DNA and RNA was formed, RNase H could bind the hybridized RNA and digest it (Figure 1). We expected that such light-activated dumbbell ODNs could be applied to photocontrol enzyme-mediated RNA digestion.

RESULTS

Design and Synthesis of Azobenzene Linked Dumbbell asODNs. Our previous works are focused on the most dramatic change in hairpin stability based on the conformation of the azobenzene photoswitching by limiting the length of the spacer units.[42,43] Herein, we hope two hairpins at two terminals of an asODN form a dumbbell structure with azobenzene as hairpin loops, which may provide new possibilities for controlling RNA binding and digestion. Thus, a series of azobenzene linked dumbbell asODNs were designed and synthesized using 4,4′-bis(hydroxymethyl)azobenzene linker as hairpin loops, as shown in Figure 2. 4,4′-Bis(hydroxymethyl)-azobenzene was readily synthesized from 4-nitrobenzylalcohol in one step as previously reported in the literature.[42,43] Based on the commonly used synthetic method of phosphoramidite monomers, 4,4′-bis(hydroxymethyl)azobenzene was protected by DMT group, followed by reaction with *N*,*N*,*N*′,*N*′-tetraisopropyl-phosphorodiamidite. The azobenzene phosphoramidite (Supporting Information Figure S1) was then introduced to dumbbell ODNs by solid-phase synthesis.

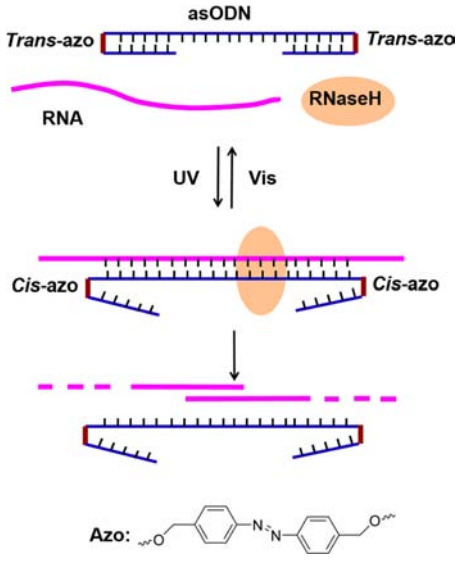

Figure 1. Strategy for photoregulating RNA digestion using azobenzene linked dumbbell asODNs. Azo: 4,4′-bis(hydroxymethyl)-azobenzene.

Az16-4: 5'-CGTTazoAACGTTTCGGACCGTAazoTACG-3'
Az16-5: 5'-ACGTTazoAACGTTTCGGACCGTAazoTACGG-3'
Az16-6: 5'-AACGTTazoAACGTTTCGGACCGTAazoTACGGT-3'
Az16-7: 5'-AAACGTTazoAACGTTTCGGACCGTAazoTACGGTC-3'
Az18-4: 5'-GTTGazoCAACGTTTCGGACCGTATazoATAC-3'
Az18-5: 5'-CGTTGazoCAACGTTTCGGACCGTATazoATACG-3'
Az18-6: 5'-ACGTTGazoCAACGTTTCGGACCGTATazoATACGG-3'
Az18-7: 5'-AACGTTGazoCAACGTTTCGGACCGTATazoATACGGT-3'
Az20-4: 5'-TTGGazoCCAACGTTTCGGACCGTATTazoAATA-3'
Az20-5: 5'-GTTGGazoCCAACGTTTCGGACCGTATTazoAATAC-3'
Az20-6: 5'-CGTTGGazoCCAACGTTTCGGACCGTATTazoAATACG-3'
Std: 5'-CCAACGTTTCGGACCGTATT-3'
Target RNA: 5'-FAM-ACAGAAAUACGGUCCGAAACGUUGGUCUGU-3'

Figure 2. Sequences of azobenzene linked dumbbell asODNs, control ODN (**Std**), and target RNA used in this study.

Generally, asODNs for highly specifically targeting mRNA require 15−30-mer oligonucleotides. Herein, antisense oligonucleotide sequences fully complementary to target RNA in these azobenzene linked dumbbell asODNs are designed to be 16 mer, 18 mer, and 20 mer long, and each hairpin contained a different length of inhibitory sense strands in two ends of these asODNs. As shown in Figure 2, the azobenzene linked dumbbell asODNs were designated to be **Az16−4**, **Az16−5**, **Az16−6**, and **Az16−7** for 16 mer asODN with 4−7 nt hairpin stems; **Az18−4**, **Az18−5**, **Az18−6**, and **Az18−7** for 18 mer asODN with 4−7 nt hairpin stems; and **Az20−4**, **Az20−5**, and **Az20−6** for 20 mer asODN with 4−6 nt hairpin stems. All these dumbbell asODNs were composed of an asODN strand and two short complementary inhibitory sense strands as binding arms at two terminals, and photomodulation of their RNA binding with complementary RNA in gel shift assay and RNase H-mediated RNA digestion were then evaluated.

Photoisomerization and Thermodynamic Stability of the Azobenzene Linked Dumbbell asODNs. The photoisomerization of azobenzene linked dumbbell asODNs under light irradiation (365 nm, 7 mW/cm^2) was investigated by UV/vis spectroscopy. In each case, the modified dumbbell asODN was thermally stable in *trans* configuration. UV irradiation led to the loss of the absorption maxima at 335 nm ($\pi-\pi^*$) and slight increase in absorption maxima at 430 nm ($n-\pi^*$). The photostationary states of *trans* to *cis* or *cis* to *trans* were achieved within 2 min although the photostationary conversion rates were slower than azobenzene itself, as shown in SI Figure

DOI: 10.1021/acs.bioconjchem.5b00125
Bioconjugate Chem. 2015, 26, 1070−1079

S2 and Figure S3. The yields of *trans* to *cis* conversion were measured immediately by native PAGE. Intensity of gel bands was used to determine the level of *trans* and *cis* isomers, given that the *trans* isomer is the sole starting material, and the percentage of *cis* isomer is the *trans* to *cis* conversion yield. After UV irradiation, *trans* to *cis* conversion yields of 68% for **Az18−4**, 71% for **Az18−5**, 63% for **Az18−6**, and 64% for **Az18−7** were thus determined (SI Figure S4). Also, thermal isomerization behavior of *cis* isomer for the dumbbell asODNs was evaluated due to thermolability of *cis*-azobenzene (Figure S5). As a result, *cis*-**Az18−4**, *cis*-**Az18−5**, *cis*-**Az18−6**, and *cis*-**Az18−7** started to isomerize above 60 °C and *cis*-**Az18−4** stably retained the *cis*-configuration up to 28 h at 20 °C, or over 8 h at 37 °C.

A change of thermodynamic stability due to isomerization of azobenzene is the necessary prerequisite to photomodulate RNA degradation. Thus, we measured the melting temperatures (T_ms) of azobenzene linked dumbbell asODNs themselves without the complementary RNA before or after UV irradiation under the same conditions, and the results were presented in Table 1 and SI Figure S6 and Figure S7. Similar to

Table 1. Melting Temperatures (T_ms) of Azobenzene Linked Dumbbell asODNs before and after UV Irradiation

	T_m (°C)		
ODNs	−UV	+UV	ΔT_m[a] (°C)
Az16−4	64.0 ± 1.3	51.2 ± 1.2	12.8
Az16−5	71.5 ± 0.5	59.4 ± 1.9	12.1
Az16−6	74.2 ± 0.8	60.1 ± 0.5	14.1
Az16−7	76.9 ± 1.4	61.4 ± 1.5	15.5
Az18−4	67.3 ± 1.2	46.0 ± 0.5	21.3
Az18−5	69.6 ± 0.6	53.3 ± 0.9	16.3
Az18−6	74.3 ± 1.2	61.4 ± 0.8	12.9
Az18−7	77.3 ± 1.0	65.2 ± 0.9	12.1
Az20−4	51.0 ± 1.6	36.4 ± 1.1	14.6
Az20−5	68.8 ± 1.5	56.0 ± 1.6	12.8
Az20−6	71.0 ± 1.5	57.2 ± 0.9	13.8

[a] $\Delta T_m = T_m$ (+UV) − T_m (−UV).

our previous work,[43] melting temperatures of the azobenzene modified dumbbell asODNs uniformly decreased when they transferred from *trans* to *cis* state and the changes of T_m in standard 1 × PBS buffer were up to 21.3 °C, which indicated that photoisomerization could be used to modulate their T_ms. In addition, when keeping the same asODN segment, the T_m values of *trans*-azobenzene modified ODNs tended to increase with increasing number of stem nucleobases at two terminal hairpins, and T_m values of their corresponding *cis* state also increased. For instance, for **Az18−4**, **Az18−5**, **Az18−6**, and **Az18−7**, the T_m values were 67.3 °C, 69.6 °C, 74.3 °C, and 77.3 °C in their *trans* states and 46.0 °C, 53.3 °C, 61.4 °C, and 65.2 °C in their *cis* states, respectively. The dumbbell structures of azobenzene modified dumbbell asODNs with higher T_m values were fully unfolded with difficulty under physiological conditions. In this case, it would lead to inefficient photoregulation of dumbbell structures, although there occurred large T_m changes along with *trans* to *cis* isomerization. But most importantly, we hope that the large T_m variation of *trans* to *cis* azobenzene dumbbell ODNs can modulate the whole dumbbell ODN structure, and thus regulate their binding to target RNA and degrade it by RNase H.

Photoregulation of Binding Target RNA with Azobenzene Linked Dumbbell asODNs. The duplex formation between asODN and sense RNA is one of the key important factors in RNA digestion. These asODNs with dumbbell structures should lead to binding competition to asODN fragments between two binding arms and their target RNA substrate. To examine the photomodulation of hybridization between target RNA and azobenzene linked dumbbell asODNs, gel shift assays were performed using native polyacrylamide gel electrophoresis. Figure 3 and Table S1 show results of three different ratios (2:1, 10:1, and 20:1) of dumbbell asODNs to a fixed amount of FAM labeled RNA (5 pmol) for each case at 37 °C. In each panel, lane 1 shows a single band corresponding to the unbound RNA alone. Lanes 2−4 and lanes 5−7 in each panel show the mobility of duplex of RNA and the dumbbell asODNs in the dark and with UV irradiation, respectively. Furthermore, lane 2, lane 3, and lane 4 in each panel correspond to the 2:1, 10:1, and 20:1 ratios of dumbbell asODNs to RNA; and lane 5, lane 6, and lane 7 also correspond to the same ratio of asODN to RNA.

As expected, panel **Std** indicated that a 20mer control ODN complementary to the middle 20 nucleotide of the 30 mer RNA was able to bind all of the RNA and form stable duplex in the dark or with UV irradiation. The azobenzene linked dumbbell asODN (**Az16−4**) with up to 20-fold excess over target RNA still only showed weak hybridization to FAM labeled-RNA in the dark, while light induced *trans* to *cis* isomerization of azobenzene clearly indicated better binding between **Az16−4** and target RNA. As the numbers of binding arms for the dumbbell ODNs (**Az16−5**, **Az16−6**, and **Az16−7**) increased one, two, or three more stem nucleobases at each terminal hairpin than **Az16−4**, the weaker binding ability of dumbbell asODNs and target RNA was observed. At the same time, photoisomerization of hairpin azobenzene did not largely increase the asODN/RNA binding. For **Az16−6** and **Az16−7** with 6- and 7-nt-long binding arms, they almost had no obvious binding to target RNA regardless of UV exposure. These results indicated that when the length of asODN fragment was fixed to 16 nt, four stem nucleobase binding arms at two terminals may possibly be used to photocontrol the binding between dumbbell asDNA and target RNA, and the photoregulation of their binding became less distinct with the increase of paired nucleobases in hairpin stems.

In order to improve photomodulation efficiency of the asODN/RNA binding, we further enhanced their binding ability by changing the length of asODN fragments complementary to target RNA or binding arms of dumbbell hairpins at their two terminals. As expected, **Az18−4**, with four stem base-pairs at two terminal hairpins and free 10 nt long complementary segment to the target RNA, could bind a small percentage of the target 30 mer RNA before UV irradiation. However, much stronger hybridization bands were observed under the same conditions upon light irradiation (Figure 3). This result was consistent with large T_m change (21.3 °C) induced by *trans* to *cis* isomerization of **Az18−4**, and indicated a clear photomodulation of duplex formation of asODN/RNA. Similarly, the binding ability of **Az18−5** with one more base-pairs in each hairpin stem to the target RNA became much higher with UV irradiation than without UV irradiation. It is worthy to note that a longer binding arm could form fewer percentages of duplexes between dumbbell ODNs and target RNA either before or after light irradiation.

DOI: 10.1021/acs.bioconjchem.5b00125
Bioconjugate Chem. 2015, 26, 1070−1079

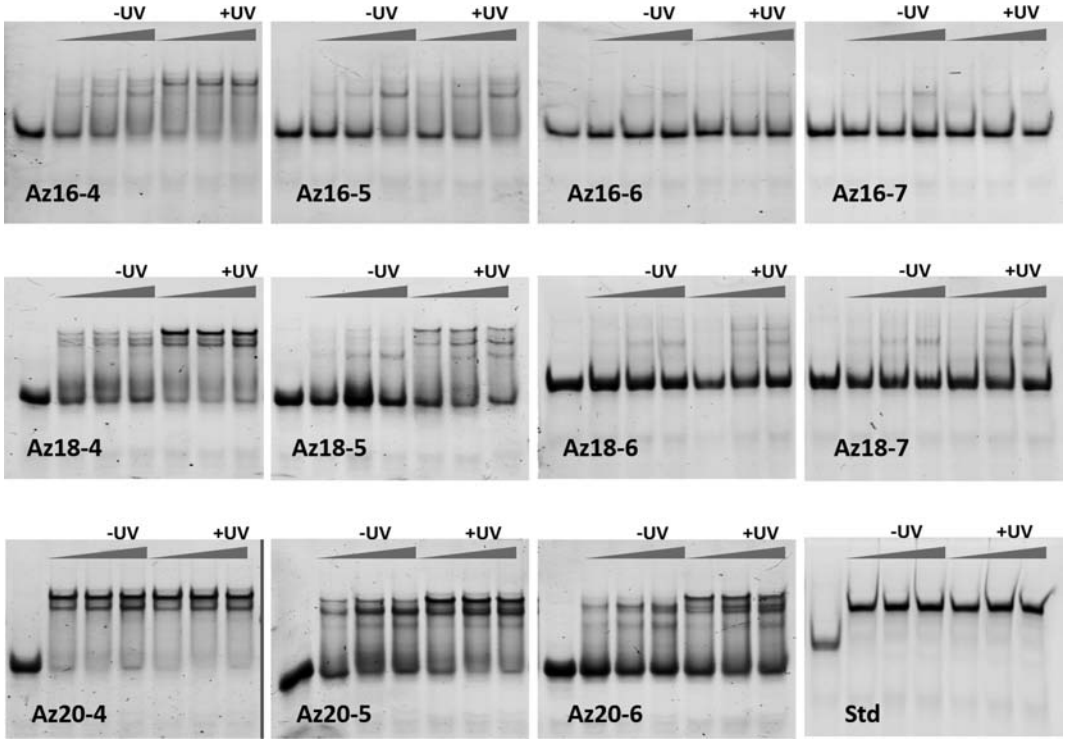

Figure 3. Native PAGE gels (20%) of the binding of azobenzene linked dumbbell asODNs (2 μM, 10 μM, and 20 μM) with the complementary FAM-labeled RNA (1 μM) in 5 μL 1 × PBS buffer after 30 min incubation at 37 °C. UV irradiation was performed for the mixture of dumbbell asODNs and FAM-RNA within 2 min.

In comparison with **Az18−4**, **Az20−4** has the same long base pairs at two terminal hairpin stems but a longer complementary segment (12 free nucleotides) for target RNA binding. Since the 12-mer duplex of ODN/RNA is relatively stable, the hybrid of **Az20−4**/RNA was efficiently formed even though no light irradiation was applied. Unlike **Az20−4**, **Az20−5** and **Az20−6** have only 10 and 8 free nucleotides available for RNA binding; partial inhibition of RNA binding was observed. At the same time, photocontrol of their hybridization with target RNA was achieved to different extents upon light exposure, respectively.

The effect of azobenzene photoswitching on RNA binding with the azobenzene linked dumbbell asODNs was also demonstrated to be reversible with UV and visible irradiation under the same conditions, which is of particular interest as the irradiated "on" and "off" states to complete dynamic optical control over biological functions. The mixture solutions of dumbbell asODNs/RNA (1:10) were exposed to UV light for 2 min and then visible light for 2 min, followed by further incubation at 37 °C for 30 min. The samples were loaded on the native gel. As expected, when subsequent visible irradiation of irradiated samples is applied, RNA binding could be restored to the initial state for all the azobenzene linked dumbbell asODNs (Figure S8).

Photoregulation of RNA Digestion with Azobenzene Linked Dumbbell asODNs. RNA cleavage by RNase H is a three-component system requiring the presence of a target RNA, a complementary asODN, and RNase H. When the complex of RNase H with RNA/asODN duplex was formed, the RNA cleavage event can happen.[44] To examine our design strategy, both azobenzene linked dumbbell asODNs and 20 mer control asODN were used to assess RNase H-mediated cleavage of a 30-mer oligoribonucleotide substrate labeled at its 5′-terminus with a fluorescein moiety (FAM). A 1:20 ratio of dumbbell asODNs to RNA substrate was chosen for the photoregulation of RNA digestion in the presence of 0.25 U RNase H for 70 min. The cleavage reactions were thus resolved, visualized, and quantified using denaturing polyacrylamide gel electrophoresis (PAGE), as shown in Figure 4

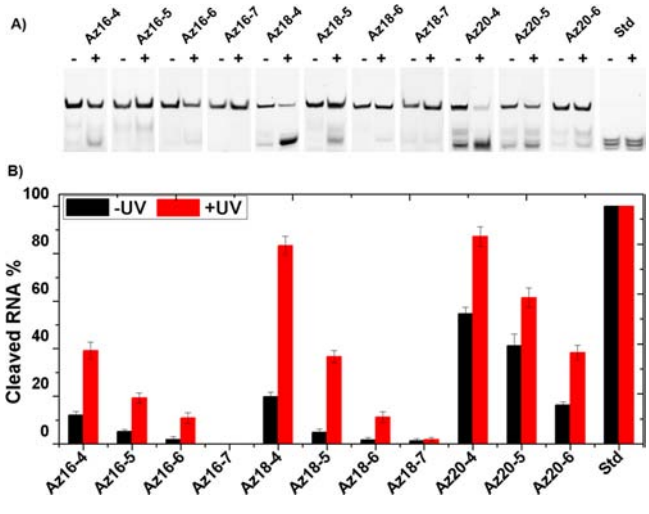

Figure 4. (A) Denaturing PAGE (20%) of photomodulaton of the RNA digestion by RNase H in the presence of 1 μM FAM-labeled RNA, 0.05 μM azobenzene linked asODNs, and 0.25 U RNase H in 25 μL RNase H buffer without or with UV irradation (365 nm, 7 mW/cm^2) at 37 °C with 70 min incubation. (B) Quantitative analysis for photoregulation of RNA digestion using all of azobenzene linked dumbbell asODNs in 25 μL RNase H buffer containing 0.25 U RNase H with 70 min incubation at 37 °C. Each set measured in more than triplicate.

DOI: 10.1021/acs.bioconjchem.5b00125
Bioconjugate Chem. 2015, 26, 1070−1079

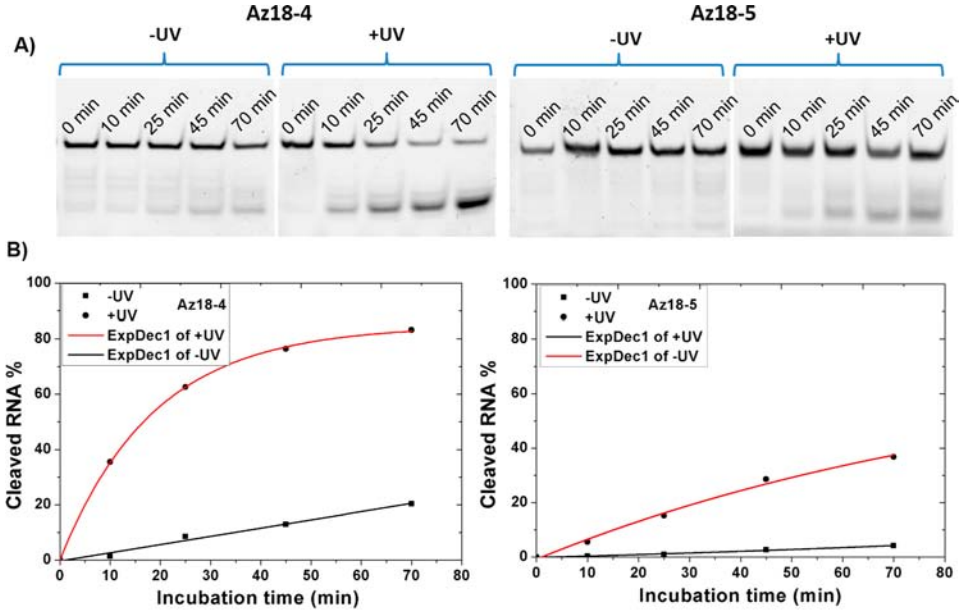

Figure 5. (A) Denaturing PAGE (20%) of photomodulaton of the RNA digestion by RNase H in the presence of 1 μM FAM-labeled RNA, 0.05 μM azobenzene linked asODNs (**Az18−4** and **Az18−5**), and 0.25 U RNase H in 25 μL RNase H buffer without or with UV irradiation (365 nm, 7 mW/cm^2) at 37 °C with increasing incubation time. Aliquots of each incubated sample were removed at 0, 10, 25, 45, and 70 min. (B) Kinetics analysis for photoregulation of RNA digestion using **Az18−4** and **Az18−5** in 25 μL RNase H buffer containing 0.25 U RNase H at 37 °C with increasing incubation time.

and SI Table S2. Under current RNase H assay conditions, no cleaved bands for RNA alone was observed; however, RNA digestion with the existence of control ODN (**Std**) was essentially completed with roughly 10 min incubation before or after UV irradiation. When the assay was performed with **Az16−4** containing 4 hairpin stem nucleobases at each end of asODN, there was 12.1% RNA digestion detectable up to 70 min incubation time (Figure 4). Light induced the *trans* to *cis* transformation of azobenzene loops, which led to about 3.2-fold increase in RNA digestion (39.3%).

In comparison with **Az16−4**, the dumbbell asODNs, **Az16−5** and **Az16−6**, have the same 16-nt-long complementary asODN sequence but the more stable dumbbell structures with 2 and 4 more base pairs in two binding arms, which led to only 6- and 4-nt-long complementary asODN segments left for target RNA binding, respectively. RNase H assay showed that both dumbbell asODNs had much lower "background" RNA cleavage (5.2% for **Az16−5**, 1.8% for **Az16−6**) than **Az16−4** before light irradiation. However, upon exposure of **Az16−5** and **Az16−6** to UV irradiation, the RNA digestion greatly increase to 19.3% for **Az16−5** and 10.9% for **Az16−6** under the same conditions, which were about a 3.7-fold and 6.1-fold increase, respectively. However, the more stable hairpin structure of **Az16−7** with two longer binding arms and two free nucleotides produced almost no "background" RNA degradation, suggesting its inability to direct RNA degradation, which was consistent with the previous report that a minimum size of four RNA/DNA base pairs is required for *E. coli* RNase H degradation at 37 °C.[45] As indicated in Figure 3, even though its two azobenzene loops were photoisomerized from *trans* to *cis* form, no binding of **Az16−7** and target RNA was observed due to the two stable binding arms. Thus, RNA digestion after UV irradiation was not observed.

Since the binding to target RNA would be enhanced with longer asODN segment of the dumbbell ODNs, we then turned to evaluate the photomodulation of target RNA digestion using azobenzene linked dumbbell asODNs with 18 mer antisense oligonucleotide fragment complementary to target RNA. For **Az18−4** with two 4-base-paired stems at both ends, the photomodulation of RNA digestion from *trans* (19.9%) to *cis* (83.5%) azobenzene loops was a 4.2-fold increase upon UV light irradiation under current RNase H assay conditions. However, the "background" RNA cleavage for **Az18−4** in the dark was a little higher. To reduce RNA digestion for *trans*-azobenzene linked dumbbell asODNs, **Az18−5** with one more nucleobase in each terminal hairpin stem and two fewer nucleobases for target RNA binding was investigated, and the result showed much better photomodulation efficiency (7.5-fold) from *trans*-**Az18−5** (4.9%) to *cis*-**Az18−5** (36.7%). Further increase of the paired nucleobases of hairpin stems further reduced RNA digestion for *trans*-azobenzene linked asODNs (**Az18−6**), but the photomodulation of RNA digestion also decreased (Table S2). As shown in Figure 4, RNA digestion for **Az18−6** with two 6-nucleotide hairpin stems was only a 7.0-fold increase from 1.6% to 11.2%, while for **Az18−7**, no difference of RNA digestion was observed before (1.4%) or after (1.9%) UV irradiation. Under the same RNase H assay conditions, **Az20−4**, **Az20−5**, and **Az20−6** with 20 nucleotide asODN fragment complementary to target RNA were evaluated for photomodualtion of target RNA digestion. **Az20−4** had high affinity to target RNA even without light-induced *trans* to *cis* transformation (Figure 3). Unsurprisingly, a high percentage of RNA digestion (54.8%) was observed for *trans*-**Az20−4** and only 1.6-fold increase of RNA digestion for *cis*-**Az20−4** after UV irradiation.

In addition, the percentage of RNase H induced RNA digestion versus the incubation time before and after light activation was evaluated in the presence of azobenzene linked dumbbell asODNs, as shown in Figure 5 and SI Figure S9 and Table S3. Typical kinetic data for target RNA cleavage were obtained by quantifying the percentage of cleaved RNA at

DOI: 10.1021/acs.bioconjchem.5b00125
Bioconjugate Chem. 2015, 26, 1070−1079

different incubation time point and fitting these data. The cleavage rate constants (k) were 2.9×10^{-3} and 0.054 min^{-1} for **Az18−4** before and after light activation with rate increase up to 18.5-fold by photoisomerization of **Az18−4**; while for **Az18−5** with lower photomodulaton ratio of RNA digestion, the rate constants of RNA cleavage were 6.3×10^{-4} in the dark and 0.0105 min^{-1} upon light activation, respectively, and light up-regulated a 16.7-fold increase in RNA digestion rate (Figure 5). Based on the kinetic data, light greatly increased RNA digestion rates for **Az18−4** and **Az18−5**, which were not fully consistent with the results of the change in the amount of RNA cleavage in 70 min (4.2-fold for **Az18−4** and 7.5-fold for **Az18−5**). This is due to the great difference in the "background" RNA cleavage for the dumbbell ODNs in the dark.

To investigate the possibility of the dumbbell ODNs for reversible photoregulation of target RNA cleavage, photoswitching RNase H-mediated RNA digestion using **Az18−4** was performed with alternate light irradiation between UV and visible light (Figure 6). The mixture of RNA and **Az18−4** was

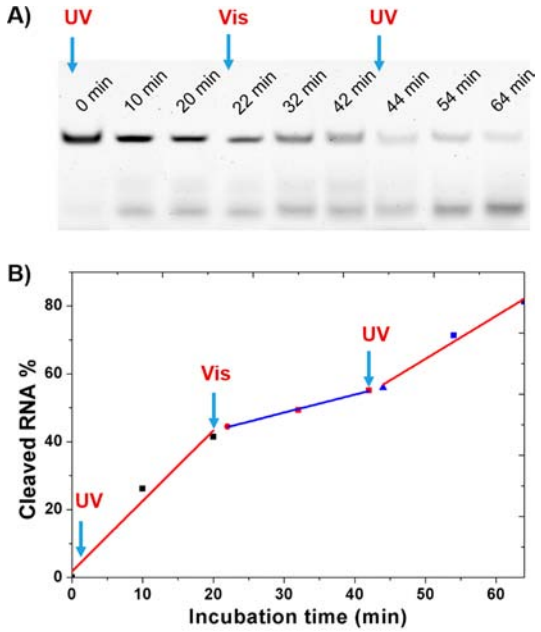

Figure 6. Photoswitching RNA digestion using **Az18−4** with alternate photoirradiation between UV (2 min) and visible light (2 min). The mixed solution of 1 μM FAM-labeled RNA and 0.05 μM **Az18−4** was incubated in 0.2 U RNase H at 37 °C, and the aliquots were collected every 10 min except for irradiation time.

irradiated with UV (2 min) and then incubated at 37 °C for 20 min in the dark. and the sample were then irradiated with visible light (2 min) and further incubated at the same condition for another 20 min, followed by UV irradiation again. Aliquots of the solution were taken out every 10 min except for irradiation time during the entire experimental process. When the mixture solution was first irradiated with UV light, RNA digestion increased sharply for the first 20 min. The percentages of RNA digestion were linearly fitted with the slope of 2.08. Upon subsequent visible irradiation and isomerization to the *trans* from *cis* form, RNA digestion slowed down significantly after following 20 min incubation, and linear fitting of the percentages of RNA digestion was observed with the slope of only 0.53. The initial RNA cleavage was partially recovered following further UV irradiation and the slope (1.27) of linear fitting data also obviously increased. This observation of light induced RNA digestion indicated that inhibition and activation of RNA digestion may be reversibly modulated through photoswitching of dumbbell asODNs by alternate irradiation with UV and visible light.

DISCUSSION

The development of photosensitive DNA conjugates to photoregulate the hybridization and RNA digestion provides the possibility of widespread applications in the regulation and investigation of gene function and expression. In related studies, photoregulation of RNA digestion was achieved with a light-activated DNA hairpin by covalently attaching a 20-mer asODN to an sODN with 12 complementary bases through a heterobifunctional photocleavable linker.[33] This study showed hydrolysis of 45% of the total 15mer RNA target after photoactivation as compared with only 4.6% for the conjugate. DNA hybridization and RNA digestion by RNase H was also previously photomodulated by using azobenzene-tethered DNA duplex.[41] By incorporating three or five azobenzene moieties to a 20-mer sense DNA strand, the amount of digested RNA after UV irradiation for the azobenzene-tethered DNA duplex was around 3-fold or 4-fold larger than in the dark, respectively. We have previously reported an easy and efficient light-activated strategy to dramatically photocontrol the structure and stability of ODN hairpins using photoisomerization of azobenzene linker as hairpin loops. This phenomenon demonstrates that this methodology can be possibly applied to the optochemical regulation of both RNA binding ability and its digestion catalyzed by RNase H.

Thus, we designed a series of photoresponsive dumbbell asODNs containing an antisense oligonucleotide fragment and two terminal hairpins with azobenzene moieties (4,4′-bis-(hydroxymethyl)azobenzene) as hairpin loops. In order to illuminate the effects on photomodulation of RNA digestion with these photoresponsive dumbbell asODNs, two important factors were considered: (1) With the same length of antisense oligonucleotides, increasing the number of nucleobases (4, 5, 6, and 7 nt) in hairpin stems will enhance their stability of two terminal oligonucleotide hairpin in order to effectively suppress the recognition of the target RNA. (2) With the same numbers of paired nucleotides in two hairpin stems, increasing the length of antisense oligonucleotide strand (16, 18, and 20 nt) will increase the numbers of free nucleotides available for target RNA binding as well as the binding energy of complementary antisense oligonucleotide fragments and target RNA. *Trans* to *cis* photoisomerization of the azobenzene linked dumbbell asODNs was determined by monitoring the absorbance of azobenzene moiety. Usually the *trans*-azobenzene as hairpin loops of dumbbell asODNs will stabilize two hairpin stems of antisense fragment with short inhibitory sense strand, while their *cis*-form hairpins will disturb the structure and stability of two terminal hairpins. This resulted in more accessibility for target RNA binding.

Melting temperature (T_m) is a thermodynamic constant to indicate the stability of two terminal hairpins. Generally, the higher the T_m of azobenzene linked dumbbell asODNs, the lower the RNA binding and RNA digestion observed for a certain length of antisense oligonucleotide strand. T_m values from *trans* to *cis* conformation decreased significantly for all azobenzene linked dumbbell asODNs with ΔT_m ranging from 12.1 to 21.3 °C (Table 1). **Az18−4** had the highest ΔT_m (21.3

DOI: 10.1021/acs.bioconjchem.5b00125
Bioconjugate Chem. 2015, 26, 1070−1079

°C) with low T_m (46.0 °C) of *cis*-**Az18−4**, which made an 18-mer antisense strand fully accessible for RNA binding and RNA digestion (83.5%) as shown in Figure 3 and Figure 4. The same things happened for **Az20−4**. However, ΔT_m values were not directly related to the photomodulation efficiencies of RNA digestion. The effects of free nucleotides in the middle of the antisense fragment available for RNA binding had to be seriously considered. *Trans*-**Az18−4** still has free unpaired 10 nucleotides that could bind the target RNA (Figure 3), which led to a high percentage of RNA digestion (19.9%) without light irradiation. Thus, only 4.2-fold enhancement of RNA digestion for RNA binding was observed for **Az18−4**. For *trans*-**Az20−4**, even much lower photomodulation efficiency (1.6-fold) was found due to more free unpaired nucleotides. However, for **Az18−5** (the second largest ΔT_m of *trans* to *cis* transformation), we could observe a 7.5-fold increase in RNA digestion with *trans* to *cis* photoisomerization of azobenzene hairpin loops. Even though RNA digestion with *cis*-**Az18−5** was less efficient than *cis*-**Az18−4** under the same RNase H assay conditions (36.7% for *cis*-**Az18−5** in comparison to 83.5% for *cis*-**Az18−4**), the percentage of "background" RNA digestion with *trans*-**Az18−5** was much less than that of *trans*-**Az18−4** (4.9% for *trans*-**Az18−5** in comparison to 19.9% for *trans*-**Az18−4**). The lower "background" RNA digestion was also due to the shorter free unpaired oligomer (8 nt). This can also explain the observations of other dumbbell asODNs that low "background" RNA digestion could be achieved with more binding stem nucleotide and fewer available unpaired nucleotides for RNA binding. In view of the variants of the dumbbell asODNs, reversibility of the photoswitching RNA digestion using **Az18−4** was demonstrated with UV−vis−UV irradiation, and enhancement or reduction of RNA digestion with azobenzene linked dumbbell ODN could be alternately achieved with UV and visible light irradiation.

CONCLUSION

In summary, a series of azobenzene linked dumbbell asODNs were designed and synthesized with 4,4′-bis(hydroxymethyl)-azobenzene moieties as hairpin loops. Photomodulation of thermodynamic stability (T_m), RNA binding, and RNase H-mediated RNA digestion were evaluated for all these photoresponsive dumbbell asODNs. These results indicated that increasing the length of paired nucleotide stems will increase the thermodynamic stability of the dumbbell asODN and its possibility of photomodulating digestion, while more free unpaired nucleotides in the middle of these dumbbell asODNs had higher affinity to target RNA and caused more RNA digestion even without UV irradiation. However, photomodulation efficiencies of RNA digestion with *trans* to *cis* transformation of these photoresponsive dumbbell asODNs were not directly related to their thermodynamic stability. In addition to the number of paired nucleobases in the hairpin stems, both the number of free unpaired nucleotides and the length of antisense oligonucleotide complementary to target RNA had a large effect on photomodulation of RNA digestion. By screening all these photosensitive dumbbell asODNs, **Az18−4** and **Az18−5** showed the best photomodulation of RNA binding and RNA digestion, and light-induced *trans* to *cis* transformation of azobenzene loops of these photoresponsive asODNs caused 4.2- and 7.5-fold increase in RNA digestion. Reversible photoregulation of RNA binding and RNA digestion was also successfully achieved using **Az18−4** when UV and visible irradiation were alternately used.

EXPERIMENTAL SECTION

General Methods, Spectral Measurements. All the reagents for organic synthesis were analytically pure and solvents for synthesis and purification were distilled over CaH_2. Silica gel column chromatography was carried out on Merck silica gel C-300. All single-stranded oligonucleotides were custom-synthesized with 1 μmol standard CPG on ABI 394 DNA/RNA synthesizer (Applied Biosystems). Deprotected oligonucleotides were purified with a Waters HPLC system using Waters reverse phase C18 column (5 μm bead, 9.6 mm × 150 mm). Mass spectra were performed by HPLC-MS apparatus with Xevo G2 Q-TOF model and recorded by ESI-MS under negative mode. The UV−visible spectra were measured on a Beckman DU800 model spectrophotometer equipped with programmed temperature controllers. Analytical PAGE was carried out on BioRad Mini-protein tetra system and imaged using ChemiDoc XRS. UV irradiation in vitro experiments were carried out using UV-LED lamp (365 nm, 7 mW/cm^2) customized from Shenzhen Langgao Technologies Co. Ltd. Visible irradiation was performed using general energy-efficient lamp (>400 nm, 11 W).

Synthesis of Azobenzene Linked Dumbbell asODNs. According to our previous report,[43] 4,4′-bis(hydroxymethyl)-azobenzene was synthesized from 4-nitrobenzylalcohol under concentrated NaOH solution. Then, one hydroxyl group of 4,4′-bis(hydroxymethyl)azobenzene was protected with 4,4′-dimethoxytrityl (DMT) group, followed by reaction with *N*,*N*,*N*′,*N*′-tetraisopropyl-phosphorodiamidite gave 2-cyanoethyl-4-*O*-{[4-(4,4′-dimethoxytrityl)-*O*-methyl-diazenyl]benzyl}-*N*,*N*′-diisopropylaminophosphoramidite. The synthesis process and the structure characterization were shown in SI Figure S1. 4,4′-Bis(hydroxymethyl)azobenzene phosphoramidite was introduced to the dumbbell ODNs by facile synthetic methods of solid phase phosphoramidite chemistry. DNA synthesis was performed using standard phosphoramidite chemistry, and standard conditions for solid-phase oligonucleotide synthesis were used for the synthesis of all oligonucleotides at a 1.0 μmol scale. Normal deoxynucleotide phosphoramidites for automated DNA synthesis were obtained from Anhui WuhuHuaren Biotechnique Co. Ltd. Standard synthetic cycles provided by Applied Biosystems were used for all normal bases using double coupling times. The azobenzene phosphoramidites without further purification were adjusted to 0.15 M solutions. Coupling times were extended to 25 min for modified nucleotides to maximize the coupling yield. The step coupling efficiencies were close to those of normal deoxynucleotide phosphoramidites.

The oligonucleotides were treated with concentrated ammonium hydroxide for 24 h at room temperature to cleave them from solid supports and deprotect the phosphates and nucleobases. The solid supports were then filtered out and the filtrates were concentrated to dryness. Oligonucleotide purification was performed by a RP-HPLC with Waters reverse phase C18 column (5 μm bead, 9.6 mm × 250 mm) using 0.05 M triethylammonium acetate (TEAA, phase A) and acetonitrile (phase B) as eluents. The samples eluted at 1.0 mL/min with running temperature at 40 °C and a gradient of acetonitrile (B): 0−30% in 20 min, 30−100% in 25 min, 100% in 30 min, 100−0% in 33 min, 0% in 35 min. The objective preparative eluent was collected after the analysis running on HPLC was monitored for UV absorption at 260 nm. All the obtained oligonucleotides were characterized by ESI-MS under negative

DOI: 10.1021/acs.bioconjchem.5b00125
Bioconjugate Chem. 2015, 26, 1070−1079

mode (1 μL sample (100 μM) in H_2O/CH_3CN (1:1) and 1% TEA). The amounts of RNA were determined by UV absorbance at 260 nm using NanoDrop (Thermo scientific).

Photoisomerization and Thermal Denaturation. Equimolar solutions of each dumbbell ODNs dissolved in 1 × PBS buffer containing 0.14 mM NaCl. The resulting solutions were heated to 90 °C and allowed to cool slowly to 15 °C. UV absorption spectra of each sample were scanned from 200 to 500 nm. In vitro photoirradiation experiments with ODN samples were achieved using UV-LED lamp (365 nm, 7 mW/cm^2) and general energy-saving lamp (>400 nm, 11 W). Sample solution was placed 2 cm away from the light source and irradiated at room temperature for 2 min. The photoreaction rate can be evaluated by checking UV absorbance at 330 nm.

Melting experiments (absorbance vs temperature) were recorded in 1 cm path-length cells using a Beckman DU800 spectrophotometer equipped with a temperature controller with a programmed step increase of 1 °C/min. Melting curves were measured at 260 nm with the same ODN concentration and the melting temperatures were determined from the peak of the first derivative plot of Absorbance at 260 nm versus temperature. T_m values were calculated from the maximum in the first derivative of the melting curves.

Binding Studies. 5′-Labeled RNA substrate with fluorescein (FAM-RNA) was purchased from GenScript Co., Ltd. (Nanjing) and redissolved in water treated with diethylpyrocarbonate (DEPC water). The sample solutions of azobenzene modified ODNs with or without 2 min UV irradiation were added to the RNA solution and incubated for 30 min. The sample solutions were exposed on 2 min visible irradiation using energy-saving lamp (>400 nm, 11 W) for samples treated with UV irradiation. The resulting solutions of the fluorescein labeled RNA (1 μM) with different concentrations of azobenzene modified ODNs (2 μM, 10 μM, and 20 μM) in 5 μL 1 × PBS buffer was used for binding assays. The mixture was incubated at 37 °C for 30 min and was then put into ice water. Before the samples were loaded into the gel, 2 μL 6× glycerol gel loading buffer containing bromophenol blue and xylene cyanol was added. All 7 μL solutions were loaded into 20% native polyacrylamide gels. The gels were then electrophoresed at 100 V for 2 h at room temperature, using 1 × TBE buffer. Gels were imaged with a ChemiDoc XRS System (Bio-Rad).

RNase H Assays. The activity of *E. coli* RNase H (Fermentas) was tested with the azobenzene linked dumbbell antisense oligonucleotides and 5′-FAM-labeled RNA (Genscript) under conditions recommended by the manufacturer (50 mM Tris-HCl, pH 7.5, 50 mM KCl, 25 mM $MgCl_2$, 0.25 mM EDTA, 0.25 mM DTT). The dumbbell ODN and 5′-FAM-labeled RNA were combined in a 1:20 ratio and incubated at 37 °C for more than 30 min to allow asODN/RNA duplex formation. As a parallel experiment on RNA degradation by RNase H after photoactivation, the ODN hairpins were added to 5′-FAM-labeled RNA, followed by illumination by UV-LED lamp for 2 min. 0.25 U of RNase H was then added to the above mixture and incubated at 37 °C. Total reaction volume was 25 μL, and the final concentrations of the ODNs and RNA were 0.05 μM and 1 μM, respectively. Aliquots were removed at various times (0 min, 10 min, 25 min, 45 min, 70 min) and quenched by heating at 65 °C for 10 min, and temporarily kept in −30 °C. All of the resulting solutions along with 2 μL gel loading buffer (50 mM EDTA, 90% formamide with bromophenol blue and xylene cyanol) were subject to electrophoresis on a 20% polyacrylamide gel containing 7 M urea. Intensity values of gel bands were integrated in Image Quant for each band with automated lane and band finding using a local method background correction in the gel lane. The relative amount of RNA digestion was determined by dividing the intensity of the band corresponding to cleaved RNA by the total intensity of the cleaved and uncleaved RNA bands.

Kinetic data for RNA cleavage in the presence of azobenzene linked dumbbell asODNs and RNase H were obtained by quantifying the percentage of cleaved target RNA at time t and fitting the data using the linear function, $[S] = A + kt$, for the dumbbell ODNs before light irradiation and a single exponential decay function, $[S] = A(1 - e^{-kt})$, for those with light irradiation, where [S] is the fraction of cleaved RNA at time t and k is rate constant of RNA cleavage.

Photoswitching RNA digestion was evaluated using **Az18−4** by incubation of RNA/**Az18−4** (20:1) in 0.2 U RNase H at 37 °C. Alternate illumination was performed by alternate UV (2 min) or visible (2 min) light illumination directly during RNA digestion reaction. Aliquots of the solution were taken out every 10 min except for irradiation time and quenched immediately for further denaturing polyacrylamide gel analysis.

■ ASSOCIATED CONTENT

Supporting Information

Supplementary Tables S1−S4, Supplementary Figures S1−S11, all the NMR spectra of synthetic phosphoramidites and their intermediates, and MS spectra of all modified ODNs. The Supporting Information is available free of charge on the ACS Publications website at DOI: 10.1021/acs.bioconjchem.5b00125.

■ AUTHOR INFORMATION

Corresponding Authors

*E-mail: heyujian@ucas.ac.cn.
*E-mail: xinjingt@bjmu.edu.cn.

Notes

The authors declare no competing financial interest.

■ ACKNOWLEDGMENTS

We are grateful for financial support by the National Natural Science Foundation of China (Grant No. 21302008, 21422201, 21272263), the National Basic Research Program of China ("973" Program; Grant No. 2012CB720600), the State Key Laboratory of Natural and Biomimetic Drugs (Grant No. K20140212, K20140204).

■ REFERENCES

(1) Rubenstein, M., Tsui, P., and Guinan, P. (2004) A review of antisense oligonucleotides in the treatment of human disease. *Drugs Future 29*, 893−909.

(2) Opalinska, J. B., Machalinski, B., Ratajczak, J., Ratajczak, M. Z., and Gewirtz, A. M. (2005) Multigene targeting with antisense oligodeoxynucleotides: an exploratory study using primary human leukemia cells. *Clin. Cancer Res. 11*, 4948−4954.

(3) Cazenave, C., Stein, C. A., Loreau, N., Thuong, N. T., Neckers, L. M., Subasinghe, C., Helene, C., Cohen, J. S., and Toulme, J. J. (1989) Comparative inhibition of rabbit globin mRNA translation by modified antisense oligodeoxynucleotides. *Nucleic Acids Res. 17*, 4255−4273.

DOI: 10.1021/acs.bioconjchem.5b00125
Bioconjugate Chem. 2015, 26, 1070−1079

(4) Kozak, M. (1986) Influences of mRNA secondary structure on initiation by eukaryotic ribosomes. *Proc. Natl. Acad. Sci. U.S.A. 83*, 2850−2854.
(5) Chi, K. N., Gleave, M. E., Klasa, R., Murray, N., Bryce, C., Lopes de Menezes, D. E., D'Aloisio, S., and Tolcher, A. W. (2001) A phase I dose-finding study of combined treatment with an antisense Bcl-2 oligonucleotide and mitoxantrone in patients with metastatic hormone-refractory prostate cancer. *Clin. Cancer Res. 7*, 3920−3927.
(6) Flaherty, K. T., Stevenson, J. P., and O'Dwyer, P. J. (2001) Antisense therapeutics: lessons from early clinical trials. *Curr. Opin. Oncol. 13*, 499−505.
(7) Luger, S. M., O'Brien, S. G., Ratajczak, J., Ratajczak, M. Z., Mick, R., Stadtmauer, E. A., Nowell, P. C., Goldman, J. M., and Gewirtz, A. M. (2002) Oligodeoxynucleotide mediated inhibition of c-myb gene expression in autografted bone marrow. *Blood 99*, 1150−1158.
(8) Shi, Y., and Koh, J. T. (2004) Light-activated transcription and repression by using photocaged SERMs. *ChemBioChem 5*, 788−796.
(9) Wang, Y., Wu, L., Wang, P., Lv, C., Yang, Z., and Tang, X. (2012) Manipulation of gene expression in zebrafish using caged circular morpholino oligomers. *Nucleic Acids Res. 40*, 11155−11162.
(10) Casey, J. P., Blidner, R. A., and Monroe, W. T. (2009) Caged siRNAs for spatiotemporal control of gene silencing. *Mol. Pharmaceutics 6*, 669−685.
(11) Yamazoe, S., Liu, Q., McQuade, L. E., Deiters, A., and Chen, J. K. (2014) Sequential gene silencing using wavelength-selective caged morpholino oligonucleotides. *Angew. Chem., Int. Ed. 53*, 10114−10118.
(12) Ando, H., Furuta, T., Tsien, R. Y., and Okamoto, H. (2001) Photo-mediated gene activation using caged RNA/DNA in zebrafish embryos. *Nat. Genet. 28*, 317−325.
(13) Young, D. D., Lively, M. O., and Deiters, A. (2010) Activation and deactivation of DNAzyme and antisense function with light for the photochemical regulation of gene expression in mammalian cells. *J. Am. Chem. Soc. 132*, 6183−6193.
(14) Zheng, G., Cochella, L., Liu, J., Hobert, O., and Li, W. (2011) Temporal and spatial regulation of microRNA activity with photo-activatable cantimirs. *ACS Chem. Biol. 6*, 1332−1338.
(15) Hemphill, J., Govan, J., Uprety, R., Tsang, M., and Deiters, A. (2014) Site-specific promoter caging enables optochemical gene activation in cells and animals. *J. Am. Chem. Soc. 136*, 7152−7158.
(16) Wu, L., Pei, F., Zhang, J., Wu, J., Feng, M., Wang, Y., Jin, H., Zhang, L., and Tang, X. (2014) Synthesis of site-specifically phosphate-caged siRNAs and evaluation of their RNAi activity and stability. *Chem.—Eur. J. 20*, 12114−12122.
(17) Wu, L., Wang, Y., Wu, J. Z., Lv, C., Wang, J., and Tang, X. J. (2013) Caged circular antisense oligonucleotides for photomodulation of RNA digestion and gene expression in cells. *Nucleic Acids Res. 41*, 677−686.
(18) Shah, S., Jain, P. K., Kala, A., Karunakaran, D., and Friedman, S. H. (2009) Light -activated RNA interference using double-stranded siRNA precursors modified using a remarkable regiospecificity of diazo-based photolabile groups. *Nucleic Acids Res. 37*, 4508−4517.
(19) Govan, J. M., Lively, M. O., and Deiters, A. (2011) Spatiotemporal control of microRNA function using light-activated antagomirs. *J. Am. Chem. Soc. 133*, 13176−13182.
(20) Ogasawara, S., and Maeda, M. (2008) Reversible photo-switching of a G-quadruplex. *Angew. Chem., Int. Ed. 47*, 8839−8842.
(21) Hohsaka, T., Kawashima, K., and Sisido, M. (1994) Photo-switching of NAD^+-mediated enzyme reaction through photoreversible antigen-antibody reaction. *J. Am. Chem. Soc. 116*, 413−414.
(22) Cahová, H., and Jaschke, A. (2013) Nucleoside-based diarylethene photoswitches and their facile incorporation into photoswitchable DNA. *Angew. Chem., Int. Ed. 52*, 3186−3190.
(23) Liu, Q., and Deiters, A. (2014) Optochemical control of deoxyoligonucleotide function via a nucleobase-caging approach. *Acc. Chem. Res. 47*, 45−55.
(24) Keiper, S., and Vyle, J. S. (2006) Reversible photocontrol of deoxyribozyme-catalyzed RNA cleavage under multiple-turnover conditions. *Angew. Chem., Int. Ed. 45*, 3306−3309.
(25) Chaulk, S. G., and MacMillan, A. M. (1998) Caged RNA: photo-control of a ribozyme reaction. *Nucleic Acids Res. 26*, 3173−3178.
(26) Liang, X. G., Asanuma, H., Kashida, H., Takasu, A., Sakamoto, T., Kawai, G., and Komiyama, M. (2003) NMR study on the photoresponsive DNA tethering an azobenzene: Assignment of the absolute configuration of two diastereomers and structure determination of their duplex in the trans-form. *J. Am. Chem. Soc. 125*, 16408−16415.
(27) Asanuma, H., Tamaru, D., Yamazawa, A., Liu, M. Z., and Komiyama, M. (2002) Photoregulation of the transcription reaction of T7 RNA polymerase by tethering an azobenzene to the promoter. *ChemBioChem 3*, 786−789.
(28) Nishioka, H., Liang, X., Kashida, H., and Asanuma, H. (2007) 2,6-Dimethylazobenzene as an efficient and thermo-stable photo-regulator for the photoregulation of DNA hybridization. *Chem. Commun. 12*, 4354−4356.
(29) Goldau, T., Murayama, K., Brieke, C., Steinwand, S., Mondal, P., Biswas, M., Burghardt, I., Wachtveitl, J., Asanuma, H., and Heckel, A. (2015) Reversible photoswitching of RNA hybridization at room temperature with an azobenzene C-nucleoside. *Chem.—Eur. J. 21*, 2845−2854.
(30) Uno, S. N., Dohno, C., Bittermann, H., Malinovskii, V. L., Haner, R., and Nakatani, K. (2009) A light-driven supramolecular optical switch. *Angew. Chem. 48*, 7362−7365.
(31) Tang, X. J., Su, M., Yu, L. L., Lv, C., Wang, J., and Li, Z. J. (2010) Photomodulating RNA cleavage using photolabile circular antisense oligodeoxynucleotides. *Nucleic Acids Res. 38*, 3848−3855.
(32) Tang, X., Swaminathan, J., Gewirtz, A. M., and Dmochowski, I. J. (2008) Regulating gene expression in human leukemia cells using light-activated oligodeoxynucleotides. *Nucleic Acids Res. 36*, 559−569.
(33) Tang, X., and Dmochowski, I. J. (2006) Controlling RNA digestion by RNase H with a light-activated DNA hairpin. *Angew. Chem., Int. Ed. 45*, 3523−3526.
(34) Szymański, W., Beierle, J. M., Kistemaker, H. A. V., Velema, W. A., and Feringa, B. L. (2013) Reversible photocontrol of biological systems by the incorporation of molecular photoswitches. *Chem. Rev. 113*, 6114−6178.
(35) Beharry, A. B., and Woolley, G. A. (2011) Azobenzene photoswitches for biomolecules. *Chem. Soc. Rev. 40*, 4422−4437.
(36) Wang, Q., Yi, L., Liu, L., Zhou, C., and Xi, Z. (2008) A thermostable azo-linker for reversible photoregulation of DNA replication. *Tetrahedron Lett. 49*, 5087−5089.
(37) Yamazawa, A., Liang, X. G., Asanuma, H., and Komiyama, M. (2000) Photoregulation of DNA polymerase reaction by oligonucleotides bearing an azobenzene. *Angew. Chem., Int. Ed. 39*, 2356−2358.
(38) Asanuma, H., Ito, T., Yoshida, T., Liang, X. G., and Komiyama, M. (1999) Photoregulation of the formation and dissociation of a DNA duplex by using the cis-trans isomerization of azobenzene. *Angew. Chem., Int. Ed. 38*, 2393−2395.
(39) Asanuma, H., Takarada, T., Yoshida, T., Tamaru, D., Liang, X. G., and Komiyama, M. (2001) Enantioselective incorporation of azobenzene into oligodeoxyribonucleotide for effective photoregulation of duplex formation. *Angew. Chem., Int. Ed. 40*, 2671−2673.
(40) Zhou, M., Liang, X., Mochizuki, T., and Asanuma, H. (2010) A light-driven DNA nanomachine for the efficient photoswitching of RNA digestion. *Angew. Chem., Int. Ed. 49*, 2167−2170.
(41) Matsunaga, D., Asanuma, H., and Komiyama, M. (2004) Photoregulation of RNA digestion by RNase H with azobenzene-tethered DNA. *J. Am. Chem. Soc. 126*, 11452−11453.
(42) Wu, L., Koumoto, K., and Sugimoto, N. (2009) Reversible stability switching of a hairpin DNA via a photo-responsive linker unit. *Chem. Commun. 14*, 1915−1917.
(43) Wu, L., Wu, Y., Jin, H., Zhang, L., He, Y., and Tang, X. (2015) Photoswitching properties of hairpin ODNs with azobenzene derivatives at the loop position. *Med. Chem. Commun. 6*, 461−468.
(44) Zamaratski, E., Pradeepkumar, P. I., and Chattopadhyaya, J. (2001) A critical survey o the structure-function of the antisense oligo/

DOI: 10.1021/acs.bioconjchem.5b00125
Bioconjugate Chem. 2015, 26, 1070−1079

RNA heteroduplex as substrate for RNase H. *J. Biochem. Biophys. Methods 48*, 189−208.
(45) Hogrefe, H. H., Hogrefe, R. I., Walder, R. Y., and Walder, J. A. (1990) Kinetic analysis of Escherichia coli RNase H using DNARNA-DNA/DNA substrates. *J. Biol. Chem. 265*, 5561−5566.

DOI: 10.1021/acs.bioconjchem.5b00125
Bioconjugate Chem. 2015, 26, 1070−1079